AD-A167 138 QUANTIFICATION OF INTERFERENCE AND DETECTABILITY PROPERTIES OF VISUAL STI.. (U) HARVARD UNIV CAMBRIDGE MA DIV OF APPLIED SCIENCES R E KRONAUER 31 JAN 86 1/1

UNCLASSIFIED AFOSR-TR-86-0248 F49620-81-K-0016 F/G 6/16 NL

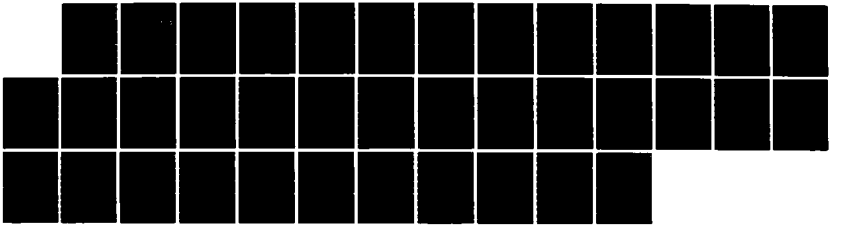

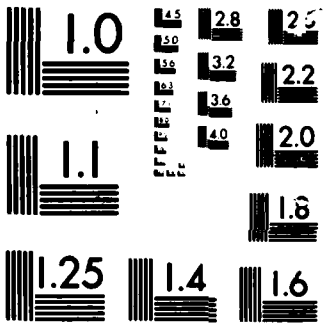

MICROCOPY CHART

(2)

QUANTIFICATION OF INTERFERENCE AND DETECTABILITY PROPERTIES OF VISUAL STIMULI FOR OPTIMAL DISPLAY DESIGN

Contract No. F49620-81-K-0016

Final Technical Report: January 1986

Submitted to:

Dr. John F. Tangney
AFOSR/NL
Washington, D. C. 20332-6448

Submitted by:

Professor Richard E. Kronauer
Division of Applied Sciences
Pierce Hall 324
Harvard University
Cambridge, Mass. 02138

Controlling Office:

USAF Office of Scientific
Research/NL
Bolling Air Force Base, D.C. 20332

UNCLASSIFIED
SECURITY CLASSIFICATION OF THIS PAGE

ADA 167138

REPORT DOCUMENTATION PAGE

1a. REPORT SECURITY CLASSIFICATION: UNCLASSIFIED	1b. RESTRICTIVE MARKINGS
2a. SECURITY CLASSIFICATION AUTHORITY	3. DISTRIBUTION/AVAILABILITY OF REPORT: Approved for public release; distribution unlimited.
2b. DECLASSIFICATION/DOWNGRADING SCHEDULE	
4. PERFORMING ORGANIZATION REPORT NUMBER(S)	5. MONITORING ORGANIZATION REPORT NUMBER(S): AFOSR-TR- 86-0248
6a. NAME OF PERFORMING ORGANIZATION: Harvard University; 6b. OFFICE SYMBOL (If applicable)	7a. NAME OF MONITORING ORGANIZATION: Air Force Office of Scientific Research/NL
6c. ADDRESS (City, State, and ZIP Code): Pierce Hall, Cambridge MA	7b. ADDRESS (City, State, and ZIP Code): Building 410, Bolling AFB, DC 20332-6448
8a. NAME OF FUNDING/SPONSORING ORGANIZATION: AFOSR; 8b. OFFICE SYMBOL (If applicable): NL	9. PROCUREMENT INSTRUMENT IDENTIFICATION NUMBER: F49620-81-K-0016
8c. ADDRESS (City, State, and ZIP Code): Building 410, Bolling AFB, DC 20332-6448	10. SOURCE OF FUNDING NUMBERS: PROGRAM ELEMENT NO. 61102F; PROJECT NO. 2313; TASK NO. A5; WORK UNIT ACCESSION NO.

11. TITLE (Include Security Classification)
QUANTIFICATION OF INTERFERENCE AND DETECTABILITY PROPERTIES OF VISUAL STIMULI FOR OPTIMAL DISPLAY DESIGN

12. PERSONAL AUTHOR(S)
Dr. Richard Kronauer

13a. TYPE OF REPORT	13b. TIME COVERED	14. DATE OF REPORT (Year, Month, Day)	15. PAGE COUNT
Final	FROM 6/81 TO 2/85	31 Jan 86	32

16. SUPPLEMENTARY NOTATION

17. COSATI CODES			18. SUBJECT TERMS (Continue on reverse if necessary and identify by block number)
FIELD	GROUP	SUB-GROUP	HUMAN VISION, PSYCHOPHYSICS, MASKING

19. ABSTRACT (Continue on reverse if necessary and identify by block number)

Masking provides information about spatial-temporal tuning of detectors. The detectability of a test sine-wave grating was measured in the presence of a mask of one or more sine-wave gratings. Patterns varied in spatial frequency, orientation and velocity. Conclusions of 4 studies are: (1) Orientation and spatial frequency tuning are not separable: changing relative mask-test spatial frequency changes orientation tuning. (2) Patterns moving in opposite directions are not detected independently; right and left moving patterns mask each other and are detected by opponent-motion mechanisms sensitive to opposite velocities. At threshold, opposite directions may be detected independently. (3) Masking of a wide range of tests by a vertical mask of 4cpd, moving left or right at 4 Hz, showed: (a) asymmetry wherein low spatial and temporal tests were strongly masked and high spatial frequencies were facilitated; (b) non-separability of the three tuning variable of spatial and temporal frequency and orientation, ruling out simple explanations. (4) A mask consisting of a small group of spectral components (simulating bandlimited 2D noise) produced strong masking by

20. DISTRIBUTION/AVAILABILITY OF ABSTRACT	21. ABSTRACT SECURITY CLASSIFICATION
☒ UNCLASSIFIED/UNLIMITED ☒ SAME AS RPT. ☐ DTIC USERS	UNCLASSIFIED
22a. NAME OF RESPONSIBLE INDIVIDUAL: JOHN F TANGNEY	22b. TELEPHONE (Include Area Code): (202) 767-5021; 22c. OFFICE SYMBOL: NL

DD FORM 1473, 84 MAR — 83 APR edition may be used until exhausted. All other editions are obsolete.

SECURITY CLASSIFICATION OF THIS PAGE
UNCLASSIFIED

TABLE OF CONTENTS

QUANTIFICATION OF INTERFERENCE AND DETECTABILITY PROPERTIES OF VISUAL STIMULI FOR OPTIMAL DISPLAY DESIGN

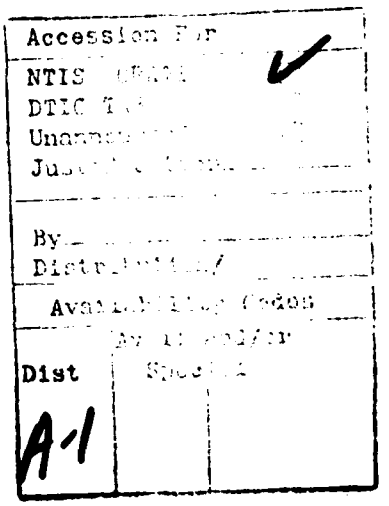

INTRODUCTION

The visual system is in many ways analogous to a collection of moderate bandwidth signal processing channels, arranged in parallel, at least insofar as early processing stages are concerned. If visual stimuli are precisely quantified in their spatial, temporal, and chromatic properties the bandwidths of the channels can be measured in terms of the interference between different stimuli. Psychophysical techniques have revealed channels that are selective for line orientation (Gilinsky, 1968), bar width or spatial frequency (Pantle and Sekuler, 1968a, Blakemore and Campbell, 1969), the direction (Sekuler and Ganz, 1963), and velocity of motion (Pantle and Sekuler, 1968b).

In masking studies the detectability of a low-contrast test stimulus is measured in the presence of a strong masking stimulus. Precise descriptions of test and masking stimuli are, we believe, best made in terms of spatial and temporal frequencies and orientations of sine-wave gratings, which then constitute the elementary stimulus components.

In the typical masking experiment, the mask and test gratings differ in only one of the several parameters. (For example, both patterns have the same, uniform chromaticity, and they both have zero temporal frequency and the same orientation and differ only in spatial frequency.) It has generally been implicitly assumed that parameters such as spatial frequency and orientation are separable variables for the visual system, i.e. the tuning function for two variables will be the product of the tuning functions for each variable separately. Our first masking study

was performed to test this unexamined orthogonality assumption, and we found it to be significantly incorrect for the variables of spatial frequency and orientation: masking bandwidths for orientation vary by a factor of two depending on the spatial frequency difference between the test and mask. We expected that the addition of a temporal frequency difference would show the orthogonality hypothesis to be further in error. One principal objective of our research was to map out the full three-dimensional masking function for gratings of matched color by differencing spatial frequency, orientation, and temporal frequency simultaneously. This project is described as Masking Study 3. One of the main findings was that masking was highly bidirectional in velocity. That is, a suprathreshold mask moving in one direction strongly reduced the visibility of a test moving in the same and opposite directions. This effect was thorougly studied, and it was shown that the visual system contains opponent motion mechanisms that are highly sensitive to the difference of opposite velocities of similar patterns (Masking Study 2). Thus opposite velocities are not detected independently, except perhaps very near threshold.

In the above studies both mask and test sine-wave grating stimuli are nonrandom (coherent single sine-wave gratings). A related and in many ways a more fundamental question arises in masking by visual noise. Extremely little information exists on this subject due in large part to technical difficulties. It is, for example, a relatively easy matter to make a single frame of a CRT display a random grating, band-limited in spatial frequency.

Also, a time sequence of statistically independent images of this kind (i.e. broadband in temporal frequency) is easy to generate. However, simultaneous band-limitation in both time and space requires extensive computation and image storage capability.

The basic results for spatial-frequency maskings, using noise with a broad temporal frequency band were obtained by Stromeyer and Julesz (1972). We have reappraised these results and concluded that noise masking can be up to 5 times more effective than coherent masking at the same contrast level. It is remarkable that this very strong difference appears to have gone unnoticed. We attempted to determine how this difference arises (Masking Study 4), using masks made up of only 6 sine-wave grating components of fairly similar spatial and temporal frequencies and orientations. These band limited punctate spectral (BLPS) stimuli were shown to resemble in appearance band-limited 2D spatial noise, and thus the BLPS stimuli were used to approximate band-limited noise masks.

In addition to the above four empirical studies two theoretical studies were also pursued (described below).

SUMMARY OF WORK

Two theoretical studies were completed, as well as four empirical studies on visual interactions pursued with a masking paradigm. Four of these studies have been published, and since they are described in the enclosed reprints, only a brief summary will be given in this report. The final two studies are complete, but have not yet been prepared for publication, and thus we shall provide a thorough summary.

THEORETICAL STUDIES

Daugman (1985) investigated two-dimensional spatial linear filters that are constrained by general uncertainty relations which limit their attainable information resolution for orientation, spatial frequency and two-dimensional (2D) spatial position. The theoretical lower limit for the joint entropy, or uncertainty, of these variables is achieved by an optimal 2D filter family whose spatial weighting functions are generated by exponentiated bivariate second-order polynomials with complex coefficients, the elliptic generalization of the one-dimensional elementary functions proposed in Gabor's famous theory of communication (Gabor, 1946). The set includes filters with various orientation bandwidths, spatial frequency bandwidths, and spatial dimensions, favoring the extraction of various kinds of information from an image. Each such filter occupies an irreducible quantal volume (corresponding to an independent datum) in a four-dimensional information hyperspace whose axes are

interpretable as 2D visual space, orientation, and spatial frequency, and thus such a filter set could subserve an optimally efficient sampling of these variables. Evidence is presented that the 2D receptive-field profiles of simple cells in mammalian visual cortex are well described by members of this optimal 2D filter family, and thus such visual neurons could be said to optimize the general uncertainty relations for joint 2D-spatial-2D-spectral information resolution. The variety of their receptive field dimensions and orientation and spatial-frequency bandwidths, and the correlations among these, reveal several underlying constraints, particularly in width/length aspect ratio and principal axis organization, suggesting a polar division of labor in occupying the quantal volumes of information hyperspace. Such an ensemble of 2D neural receptive fields in visual cortex could locally embed coarse polar mappings of the orientation-frequency plane piecewise within the global retinotopic mapping of visual space, thus efficiently repesenting 2D spatial visual information by localized 2D spectral signatures.

In the second study Kronauer and Zeevi (1985) examined the extensive processing and reorganization of information required as retinally generated signals flow centrally. Insight into some principles of the reorganization and transformations that occur in the early stages of the visual pathway, prior to the higher stages of pattern recognition, is provided by analysis of receptive fields and cell counts. The rate of information flow is reduced by a retinal position-dependent (inhomogeneous) spatial sampling scheme about 100-fold. This principle of specialization, or

nonuniform processing, is further elaborated in the retino-cortical mapping. In the central fovea, where the retinal spatial sampling rate is the highest and processing function is uniform, there are about 4000 striate cortical neurons receiving information from each one. This number, which provides a measure of function multiplicity, drops to about 200 over the range of the near periphery. In the peripheral field beyond eight degrees, where information is compressed at the retina, the functional multiplicity stays approximately constant at 200. As it seems that no two cells perform exactly the same operation, it is concluded that the striate cortex performs many simultaneous functional mappings. Only a partial description of these various schemes of signal processing is deducible from present data, thus highlighting the challenge associated with understanding how the central nervous system constructs a meaningful representation of the visual world.

EMPIRICAL STUDIES

Three empirical studies measured pattern interactions in a simultaneous coherent masking pardigm. Both the mask and test patterns were single sine-wave gratings that could be varied in orientation, spatial frequency and velocity. The fourth study employed an incoherent mask forming a spectrally compact mask that visually resembled band-limited random noise.

Masking Study 1

Daugman (1984) measured the properties of human spatial visual channels in two-dimensional form by a signal detection masking pardigm. *Tuning surfaces* of contrast threshold elevation induced by a sinusoidal mask were generated for four Subjects, interpolated *from an* 11 × 11 Carestian grid over the Fourier plane, and numerically Fourier transformed in two dimensions to infer putative filter profiles in the 2D space domain. The mask was a constant 8 cpd vertical sine-wave grating and the test was a single sine-wave grating of varied spatial frequency and orientation. Among the main findings in the 2D frequency domain were: (1) threshold elevation surfaces are highly *polar nonseparable* -- they cannot be described as the product of a spatial frequency tuning curve times an orientation tuning curve. (2) Iso-half amplitude contours of the spectral tuning surfaces have a length/width elongation ratio of about 2:1. (3) Necessarily, resolution for spatial frequency and for orientation are in fundamental competition with 2D spatial resolution. By

calculating the occupied area of the inferred filters both in the 2D space domain and in the 2D frequency domain, it was estimated that these mechanisms approach within a factor of 2.5 of the theoretical limit of joint resolution in the two 2D domains that can be derived by 2D generalization of Gabor's famous theory of communication. Other classes of 2D filters, such as an ideal 2D bandpass filter, have joint 2D entropies which are suboptimal by a factor of 13 or more. Subject to the inherent constraints of inference from these 2D masking experiments, the evidence suggests that 2D spatial frequency channels can be described as elongated 2D spatial wave-packets which crudely resemble optimal forms for *joint information resolution* in the 2D spatial and 2D frequency domains.

Masking Study 2

Stromeyer *et al.* (1984) examined the question of whether two sine-wave gratings that move in opposite directions are processed independently. Levinson and Sekuler (1975) showed that at threshold, oppositely moving patterns may be detected independently by separate unidirectionally-sensitive mechanisms. We examined the response of these mechanisms at suprathreshold levels with a masking paradigm to see if there exists opponent-movement mechanism.

A vertical grating that sinusoidally reverses contrast can be synthesized from two identical component gratings that move with equal velocities in opoposite directions (leftward and rightward). Such a counterphase grating was used as a suprathreshold masking

pattern. When the mask was of low spatial frequency and modulated rapidly, a test pattern consisting of an increment of the rightward component and equivalent simultaneous decrement of the leftward component was highly detectable compared with simultaneous increments or decrements of both components. The visibility of the opponent-movement test signal was strongly facilitated by high-contrast masks. This facilitation was accompanied by a high sensitivity for judging the direction of motion of the test. The results showed that certain detection mechanisms are highly sensitive to the *difference* of the rightward and leftward components. However, when the mask was of threshold contrast, the rightward- and leftward-moving test components appeared to be detected independently. A high-contrast grating that rapidly moves in one direction strongly masked gratings moving in the same or opposite direction. Thus moving patterns are not detected by unidirectional mechanisms when contrast is clearly suprathreshold. The results could be explained by a model with mechanisms that are excited by one direction of motion and inhibited by the opposite direction.

Masking Study 3

The first two masking studies empoyed mask and tests of limited dimensionality. The first study employed *stationary* grating in which the relative spatial frequency and orientation of the mask and test was varied. The second study employed gratings moving in opposite directions with the same spatial frequency and vertical orientation. The third (unpublished) study

attempted to measure a full 3D masking tuning function, which will be presently described. The main results of the first two studies were confirmed: namely, (1) spatial frequency and orientation tuning were non-separable, and (2) patterns moving in opposite directions showed strong masking interactions, implying that opposite directions of motion are not processed independently.

Visual channels as inferred by the masking paradigm are known to be tuned for spatial frequency, orientation, and temporal frequency, but these tuning functions are not independent. Ever since the concept of channels was first developed in reference to masking phenomena (Campbell and Kulikowski, 1966), these tuning variables have been treated separately or in pairs but never has a full 3D masking tuning function been obtained in spatio-temporal frequency space. In order to obtain the full 3D masking characteristic we employed a two-alternative-forced-choice (2AFC) staircase in which a vertical travelling sine-wave of 4 cpd, 8 Hz, and 20% contrast masked a test sine-wave of different spatial and temporal frequencies and orientations. By finding the contrast at which a particular test wave is detectable 71% of the time in the presence of the mask compared with the unmasked threshold of the test, we were able to map out for two subjects the threshold elevation tuning surface as a function of all three spatio-temporal variables simultaneously.

Figure 1 shows the isomasking congtours for subject JM in the two-dimensional, $\theta = 0$ cut in 3D space. (For $\theta = 0$, i.e. $\omega_y = 0$). The mask coordinates are indicated by the stars. Test coordinates for which ω_x and ω_t have opposite sign are waves which move in

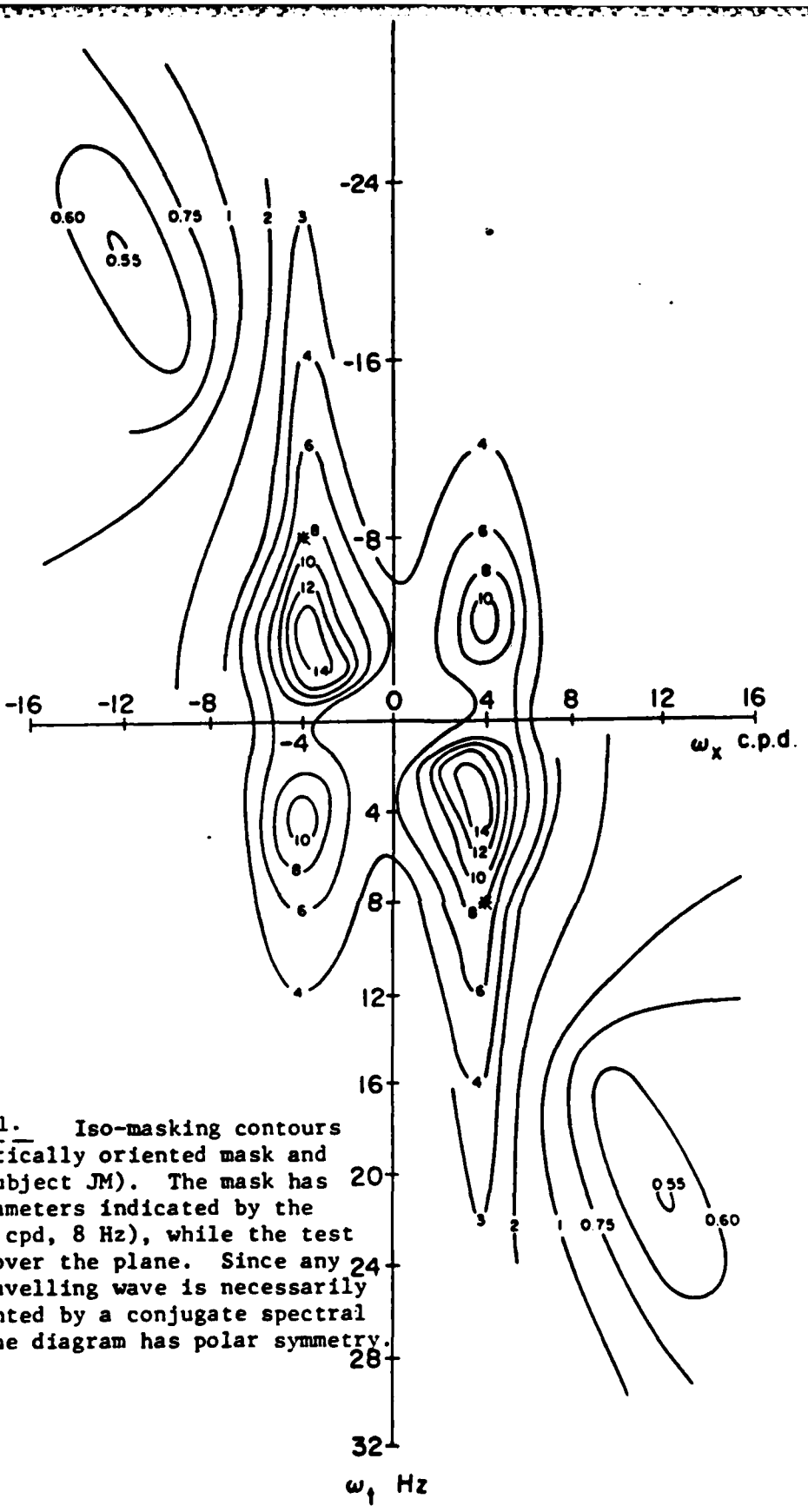

Figure 1. Iso-masking contours for vertically oriented mask and test (Subject JM). The mask has the parameters indicated by the star (4 cpd, 8 Hz), while the test varies over the plane. Since any real travelling wave is necessarily represented by a conjugate spectral pair, the diagram has polar symmetry.

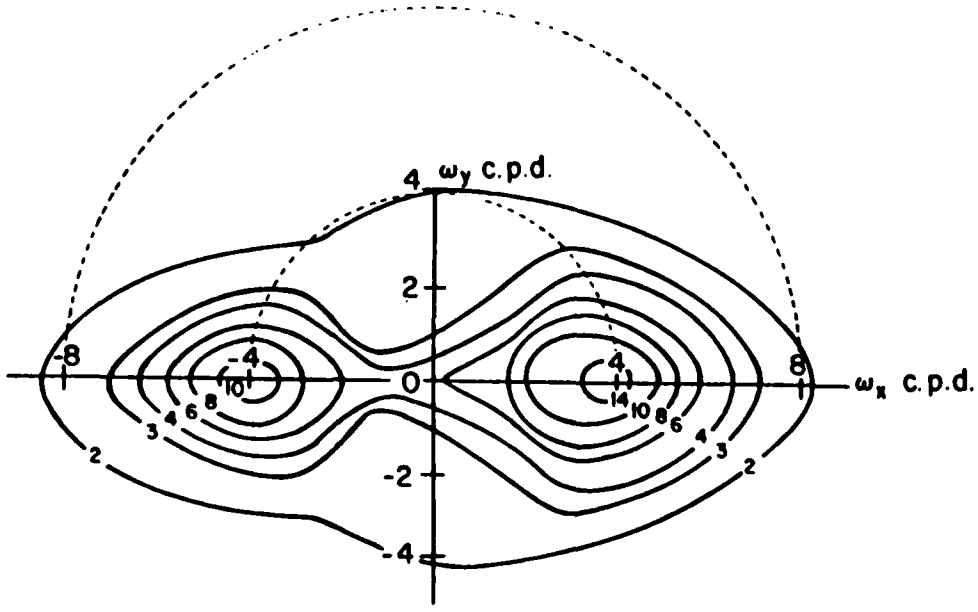

FIGURE 2. Iso-masking contours for a vertically oriented mask (4 cpd, 8 Hz), and test waves of various ω_x and ω_y at ω_t = 4Hz (subject JM). The orientation and spatial frequency of the test waves are given by:

$$\omega_s = (\omega_x^2 + \omega_y^2)^{1/2}$$

and $$\theta = \arctan(\omega_y/\omega_x).$$

The dashed circular arcs correspond to ω_s = 4 cpd and 8 cpd. Symmetry about the horizontal axis reflects an assumption that psychophysical orientation tuning effects are the same for positive and negative relative angles between mask and test.

Figure 3. Iso-masking Contours for subject TR
Conventions as in Figure D-1.

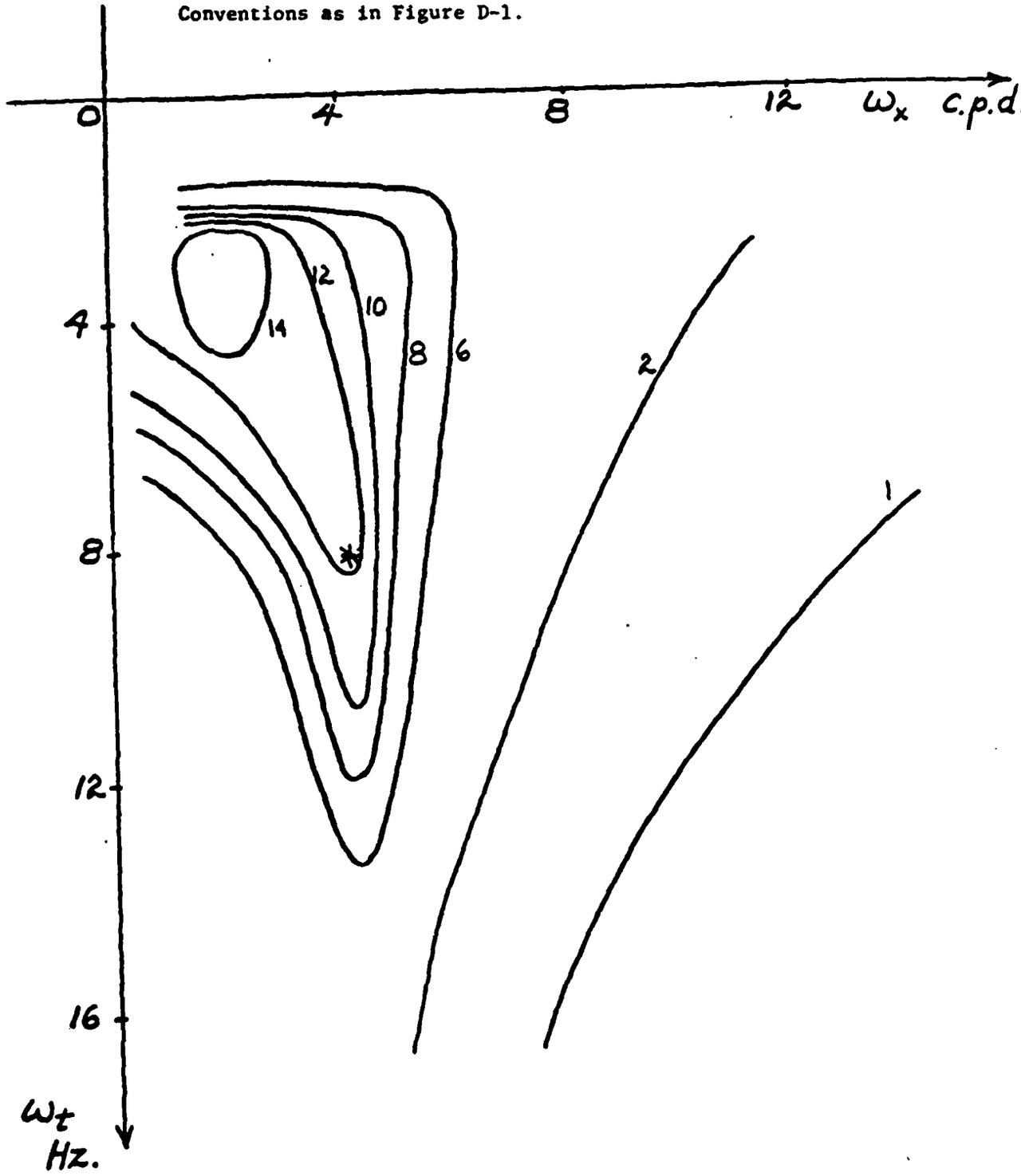

the opposite direction from the mask but which have the same vertical orientation. Figure 2 shows the iso-masking contours for the same subject in the two-dimensional cut: ω_t = 4 Hz. This temporal frequency contains the peak of the masking function (which is only half the ω_t of the mask). Figure 3 is similar to Figure 1 but for the subject TR. While these two figures are qualitatively similar they are sufficiently different that it would be misleading to average them. For both subjects the peak masking factor is greater than 14, but for TR the temporal and spatial frequencies at which this occurs are signficantly lower.

For subject JM there are two moderately compact regions in frequency 3-space in which masking is strong (ignoring conjugate quadrants), and these two regions corespond to rightward and leftward moving vertical test sine-waves. Dependence on temporal frequency is strongly asymmetrical; a test temporal frequency below that of the mask suffers much more interference than a counterpart above the mask. Remarkably, the peak threshold elevation occurs for test spatial frequencies and temporal frequencies that are roughly *half* those of the mask. The prominence of such *off-center peak masking* creates a fundamental problem for the classical channels concept, in the sense that one is hard-pressed to acocunt for this effect in terms of an ensemble of simple bandpass tuned lienar mechanisms.

Classical results for stationary mask and test gratings (Legge and Foley, 1980; Stromeyer and Julesz, 1972) give a peak masking factor at the mask condition and an approximtely symmetrical masking function in log-frequency coordinates. It is

clear that the addition of a dynamic constitutent (i.e. non-zero temporal frequency) makes a profound change. This is reinforced in our present data by the fact that the masking factor has a local minimum when the temporal frequency of the test grating is very low.

In the present study, bidirectionality of masking (for oppositely moving mask and test) is strong, yielding about 70% as much threshold elevation as codirectional masking. Strong bidirectionality was also observed in Masking Study 2. The approximate location of the local minimum between these two regions of high masking corresponds to zero spatial and temporal frequency.

Another major feature of the coherent masking surfaces is the existence of *facilitation* (threshold reduction, rather than elevation) when the spatial and temporal frequencies of the test wave are above approximately twice those of the mask. The location of the peak facilitation effect in spatio-temporal frequency space may depend on the mask contrast, as Legge and Foley (1980) found in their one-dimensional 'cut' of the masking function along the spatial frequency axis. Perhaps the familiar dipper shape of the facilitation effect's dependence on mask contrast dictates the location in 3D frequency space at which peak facilitation occurs, corresponding to a mask "equivalent contrast" (efficacy) of about 1% for matched mask and test frequencies.

The orientation tuning of the 3D masking function is comparable to that found by Daugman (Masking Study 1) for 2D stationary masking functions, but for increasing temporal

frequency the orientation tuning broadens and there is significant masking at the perpendicular. The earlier finding (Study 1) of strong polar non-separability (into a product of spatial frequency and orientation tuning curves) is strongly confirmed here, and generalized to non-separability in temporal frequency. Thus, although one speaks traditionally of a spatial frequency masking tuning function, an orientation tuning function, and a temporal frequency tuning function, in point of fact these variables are strongly interwoven and the properties of any one function depend on the values of the other variables.

In summary, the major properties of coherent masking which we have quantitatively characterized include:

- *asymmetry:* Mechanisms tuned for the detection of low temporal frequencies are strongly influenced by considerably higher mask temporal frequencies.
- *off-center peak masking:* Masking is most efficacious at spatial and temporal test frequencies considerably below those of the mask.
- *bidirectionality*: Oppositely moving components mask each other significantly, generating bimodal tuning surfaces with approximate mirror symmetry.
- *facilitation:* Certain higher spatio-temporal frequencies are significantly more detectable in the presence of the mask than they are otherwise.
- *non-separability:* The three tuning variables of spatial frequency, orientation, and temporal frequency, show strong interactions which rule out any simple

decomposition of the masking efect into separate dependencies.

Masking Study 4

We now turn to our study on incoherent masking. The test, as before, is a single sine-wave grating. The mask is a small collection of sine-wave gratings defining a compact volume in the 3D space of spatial and temporal frequency and orientation. Such a mask was deliberately chosen since it is easy to generate and specify, and, more importantly, our preliminary studies showed that such a punctate spectrum can be perceptually indistinguishable from random band-limited spatial white noise.

We must first then review this preliminary study in which we show that band limited punctate spectral (BLPS) stimuli may appear similar to the band-limited noise. Surprisingly small numbers of discrete 2D spatial Fourier components, added together, can simulate anisotropic 2D bandlimited spatial white noise. It is significant that under these circumstances the visual system cannot distinguish between a signal of very small dimension (the 5 or 6 components in the punctate spectrum) and a signal with virtually infinite dimension.

As with any equivalence class, the criteria which must be satisfied for this perceptual equivalence are revealing. We have noted the following requirements for the density and moments of the punctate spectral distribution:

(1) The punctate spectral components must be separated from each other by at least the characteristic spectral

dimensions associated with the spatial aperture through which the texture is viewed.

(2) The punctate spectral components must fall within the canonical spectral dimensions of a 'channel', namely about 1.5 octaves radially and 20 degrees angularly, as obtained from psychophysical masking and adaptation studies.

(3) The distribution of spectral components should avoid repetitions of orientation or spatial frequency.

(4) Large skew moments (diagonality) should be avoided in the spectral distribution, as should other kinds of regularity or inhomogeneity.

(5) The spectral points must not lie on or near any set of parallel equi-distant lines which include the origin, as this would lead to 2D periodicity in the space domain.

With these distribution contraints, we generated several families of BLPS stimuli comprising 3,4, ... 9 punctate spectral components sampled at random by Graeco-Latin Squares (polar grids), and we conducted discrimination experiments to find out the limits of the visual system in separating the components. We asked subjects to make pairwise judgements of complexity between the two sampled textures, by identifying which of the two contained more components. (Although the members of each pair contained different numbers of components, all images had equal rms contrast.) The results of such judgements by three subjects when comparing N versus N+L component-textures are shown in Figure 4. There is clearly an ogival psychometric function for the three

Figure 4. Complexity Discrimination for BLPS Images Differing by 1 in the Number of Components.

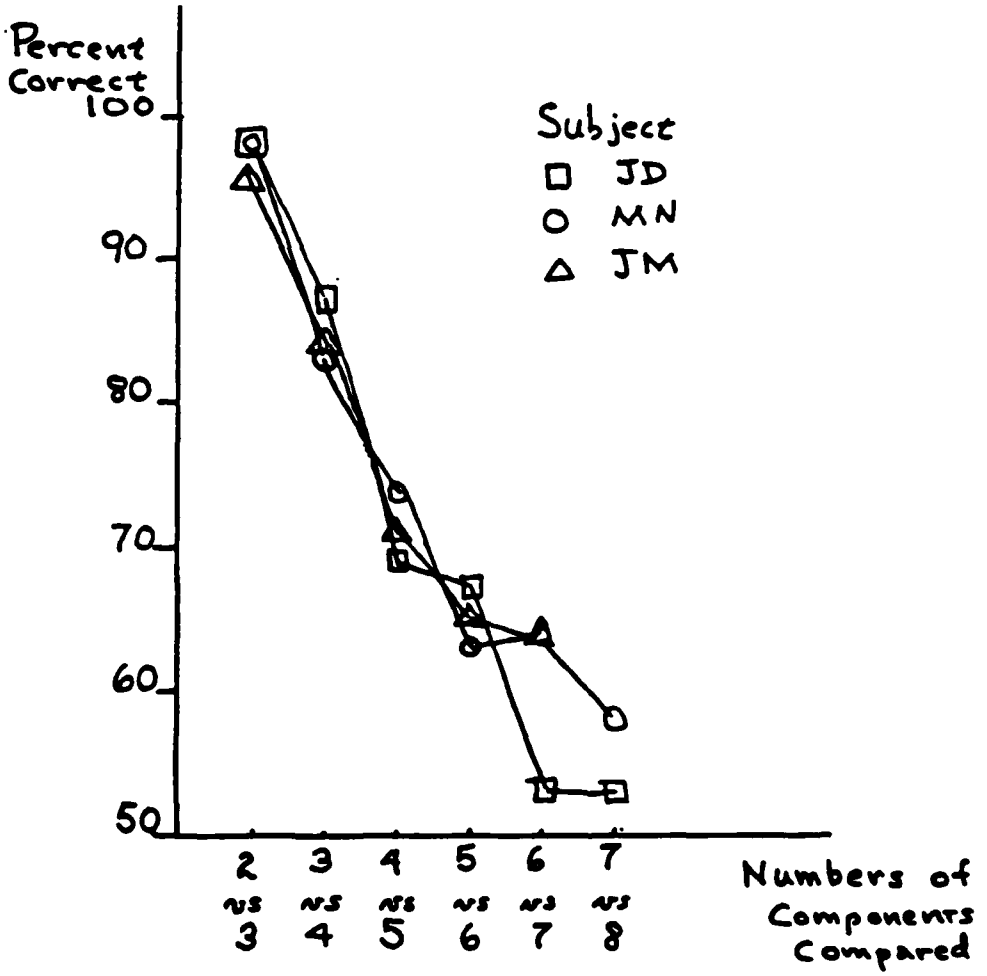

Figure 5. Complexity Discrimination for BLPS Images Differing by 1,2, or 3 in the Number of Components.

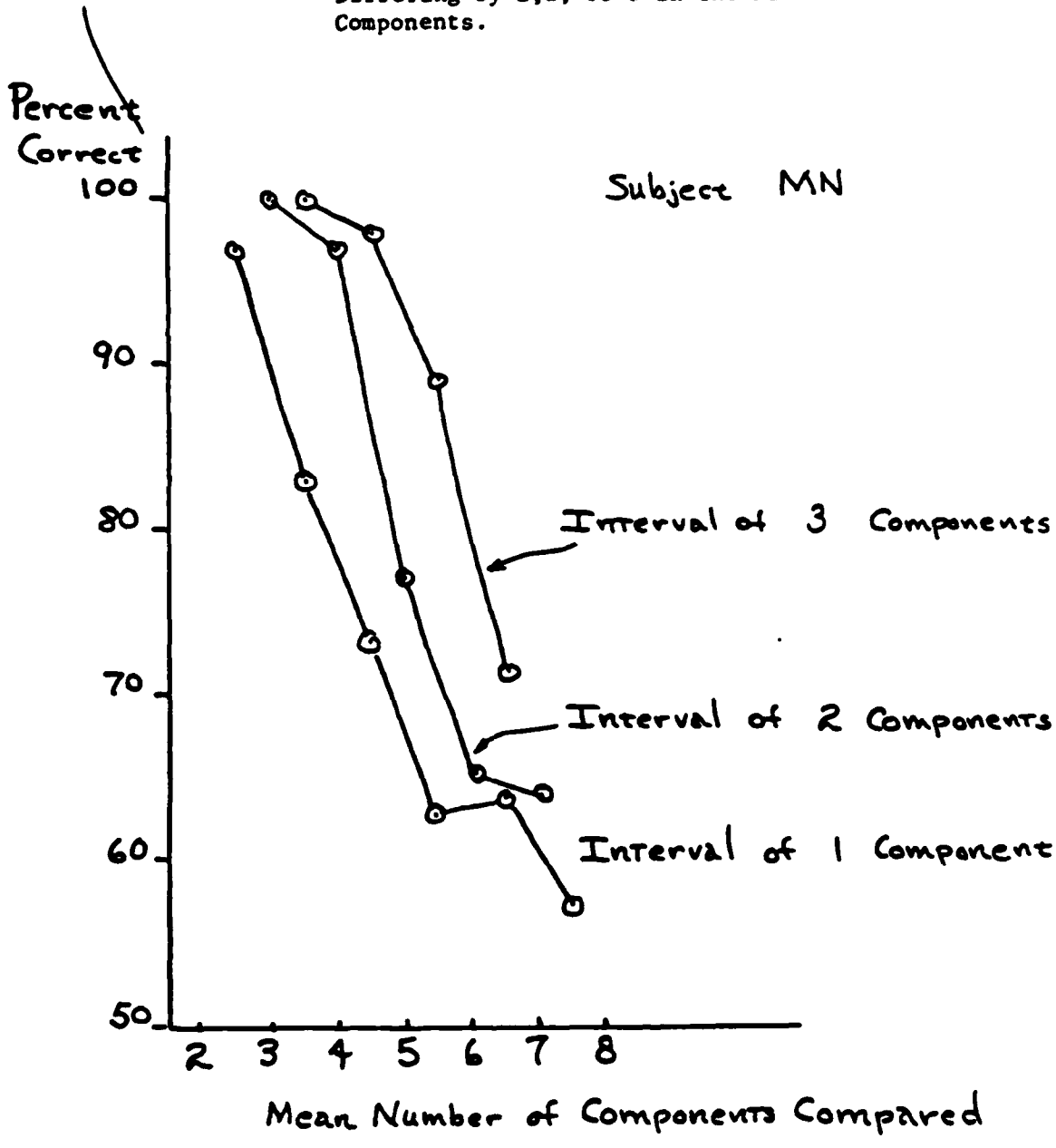

subjects, with performance falling to 70% correct responses when comparing 4 versus 5 components, and approaching the asymptotic guessing rate of 50% correct responses by the time 6 or 7 components are involved. Similar results were obtained in the N versus N+2 and N+3 tasks, as shown in Figure 5, with an expected translation in the performance curves toward higher complexities when the interval of complexity is greater. These performance curves point to a kind of colorimetry theory of texture perception, inasmuch as all textures comprising six or more components within the psychophysical band-area will form a perceptual equivalence class.

In the incoherent masking study, we employed such BLPS masks comprised of 6 sine-wave components. The rms contrast of the mask was 11%; thus each component had a contrast of $11/\sqrt{6}$ %, or 4.5%. The centroid of the mask was 5.25 cpd, 0° (vertical) orientation and zero temporal frequency. The mask components were approximately evenly spaced within a square grid in Cartesian coordinates (ω_x, ω_y). The single sine-wave test was identical to the centroid. Masking was measured with the same 2AFC psychophysical procedure employed in the previous study. The phase of the mask components was varied randomly between trials; hence each mask image was different and there was an incoherent phase relationship between test and mask.

We first examined whether such BLPS masks, which resemble in appearance band-limited spatial noise, would produce "supermasking", that is, produce masking much stronger than a coherent mask equivalent to the centroid of the BLPS mask. Masking

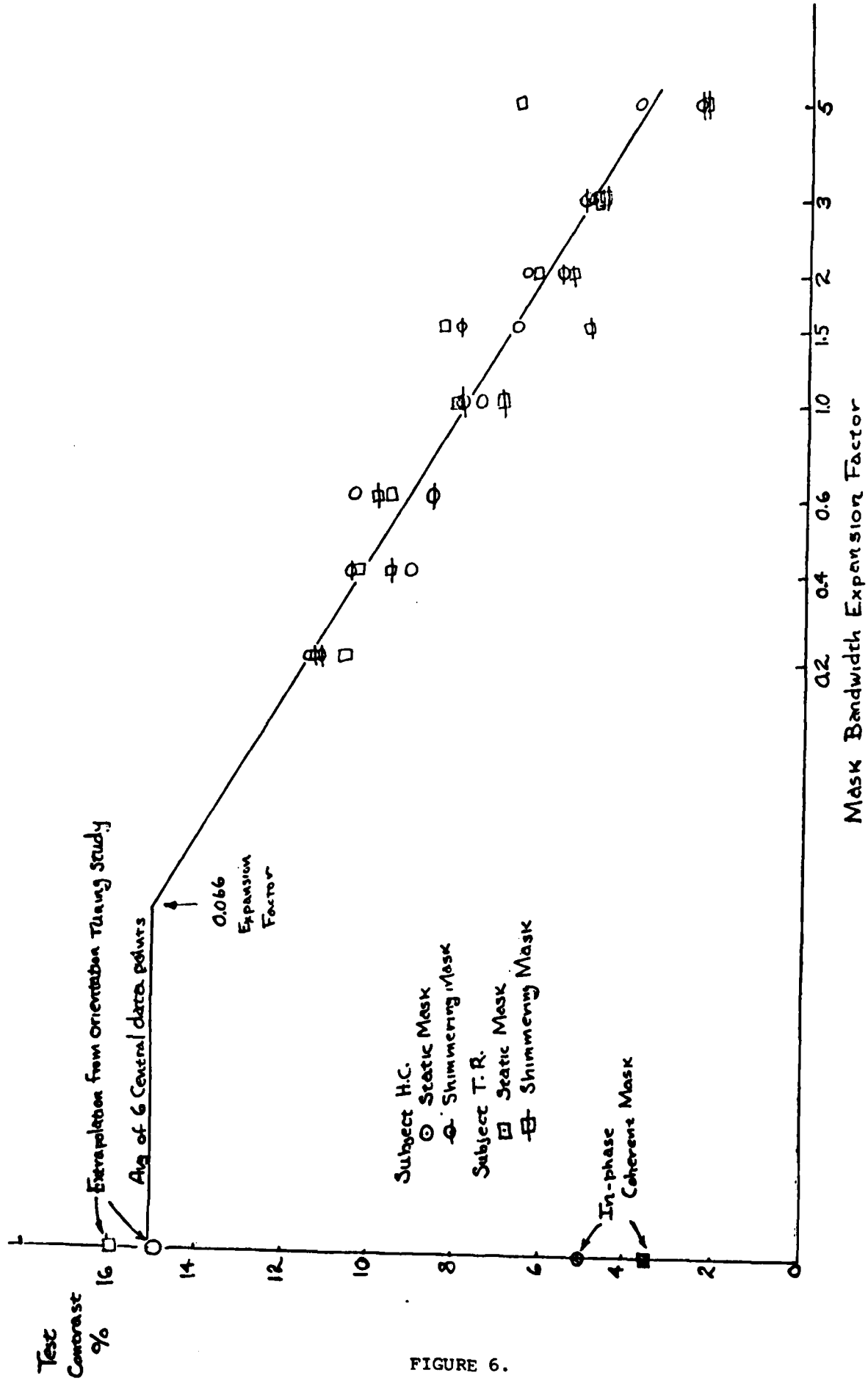
Test Contrast %
16
14
12
10
8
6
4
2
0
Extrapolation from orientation tuning study
Avg of 6 Central data points
0.066 Expansion Factor
Subject H.C.
Static Mask
Shimmering Mask
Subject T.R.
Static Mask
Shimmering Mask
In-phase Coherent Mask
0.2
0.4
0.6
1.0
1.5
2
3
5
Mask Bandwidth Expansion Factor

FIGURE 6.

was measured with 2 observers as a function of the bandwidth of the BLPS mask. The vertical axis in Figure 6 represents the threshold contrast of the test in the presence of the mask. The horizontal axis represents the mask normalized mask bandwidth, where 1.0 indicates an orientation bandwidth of ±10° and a spatial frequency bandwidth of ±0.22 octaves (i.e.±17% of the center frequency). The straight, sloped line shows that masking is reduced as the mask bandwidth is increased. The higher points on the ordinate axis represent masking for the limiting case when the bandwidth is reduced so that the mask becomes a single sine-wave grating. To obtain this point, the relative *phase* of mask and test was *randomly* varied between trials; hence there was no coherence between test and mask. The straight horizontal line extended rightwards from this point intersects the sloped line approximately at a bandwidth value of 1/a, the bandwidth owing to the limited field aperture, a = .05 radius of visual angle. Thus the masking is seen to increase with the narrowness of the mask bandwidth down to approximately the narrowest distinguishable bandwidth within the image aperture. The lower points on the ordinate axis show that the masking is very much reduced for the coherent case, in which mask and test are identical and summed in cosine phase. Thus the results show that incoherent masks produce much stronger masking than do coherent masks of equivalent rms contrast, and that in the incoherent case the masking varies inversely with mask bandwidth. Another interesting feature is that the incoherent masking is largely unaffected by whether the mask is stationary (square and circles, Figure 6) or shimmering

(squares and circles with horizontal lines) with a mean absolute temporal frequency of 1.46 Hz and zero net velocity.

In the above results, maximal masking was obtained with the incoherent mask of smallest bandwidth. We next measured 2D tuning employing such a fixed mask and a test that was varied relative to mask. The mask was a single sine-wave grating of 5.25 c/deg, 0° orientation and 11% contrast. The spatial phase of mask and test was varied randomly between trials. The results in Figure 7 show that the masking drops very rapidly when the test is only slightly different from the mask. Masking falls to half-value for tests that are approximately ±0.21 and 2.5 × ±0.21 cpd different in spatial frequency from the mask for observers H.C. and T.R. respectively, which corresponds to ±4% and ±10% of the mask spatial frequency, respectively. The similar half-bandwidth for the orientation dimension (θ) measured in radians is about 2/3× the spatial frequency half-bandwidth measured in %. We suspect, according to observers' comments, that the tuning bandwidth is so narrow because a slight difference between test and mask cause 2D beats to appear in the combined pattern. That is to say, the combined mask-plus-test appears perceptibly modulated in contrast over the region of the aperture. In contrast, when the mask and test are identical in orientation and spatial frequency, the content is uniform over the aperture and there are no beats to provide clues as to the presence of the test.

The above results show that when the mask is very narrow-band the masking tuning function is sharp, presumably because beats strongly aid detection when the test is only slightly different

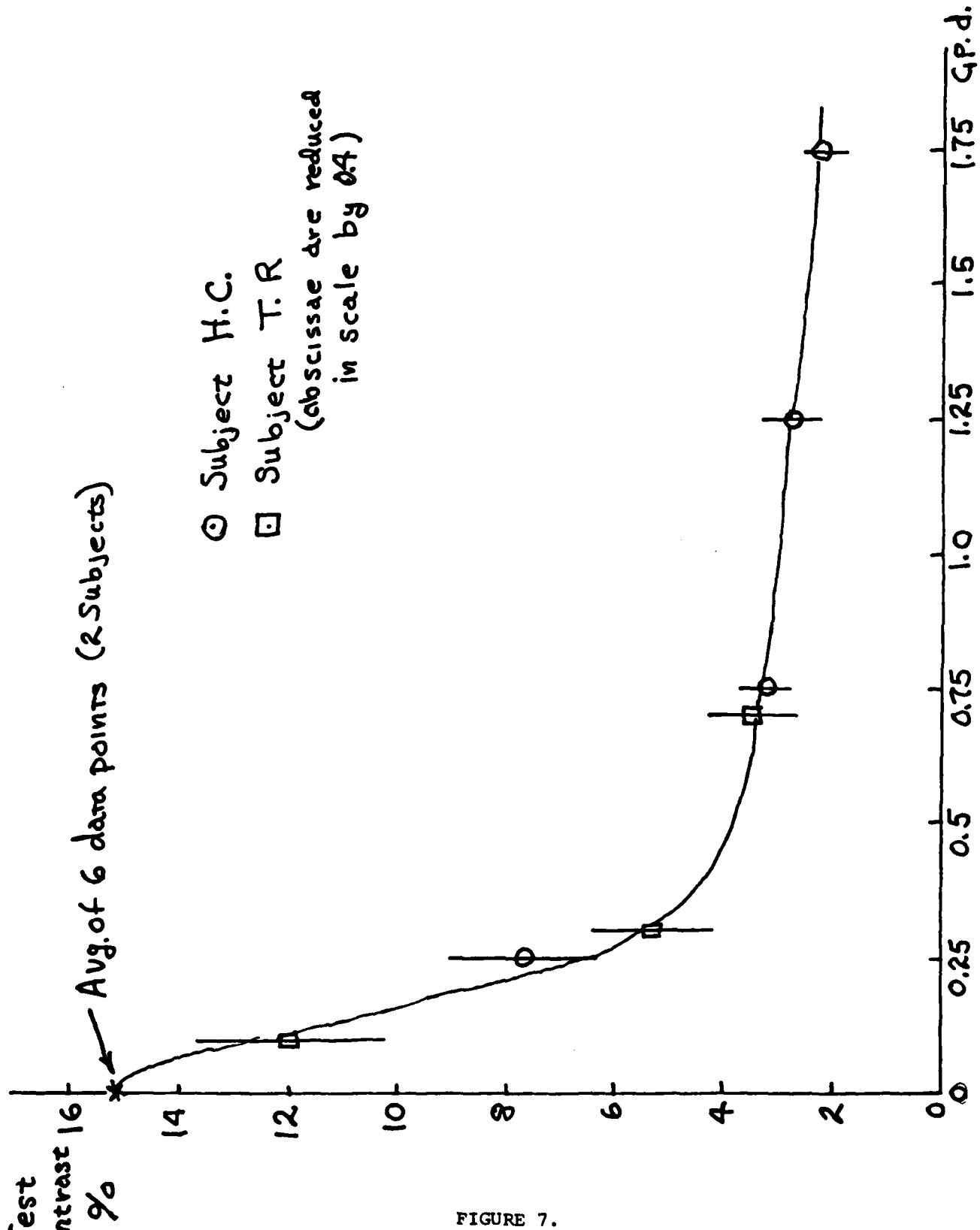
Test Contrast %
16
14
12
10
8
6
4
2
0
Avg. of 6 data points (2 Subjects)
⊙ Subject H.C.
⊡ Subject T.R
(abscissae are reduced in scale by .04)
0
0.25
0.5
0.75
1.0
1.25
1.5
1.75 C.P.d.
Mask-Test Spatial Frequency Difference

FIGURE 7.

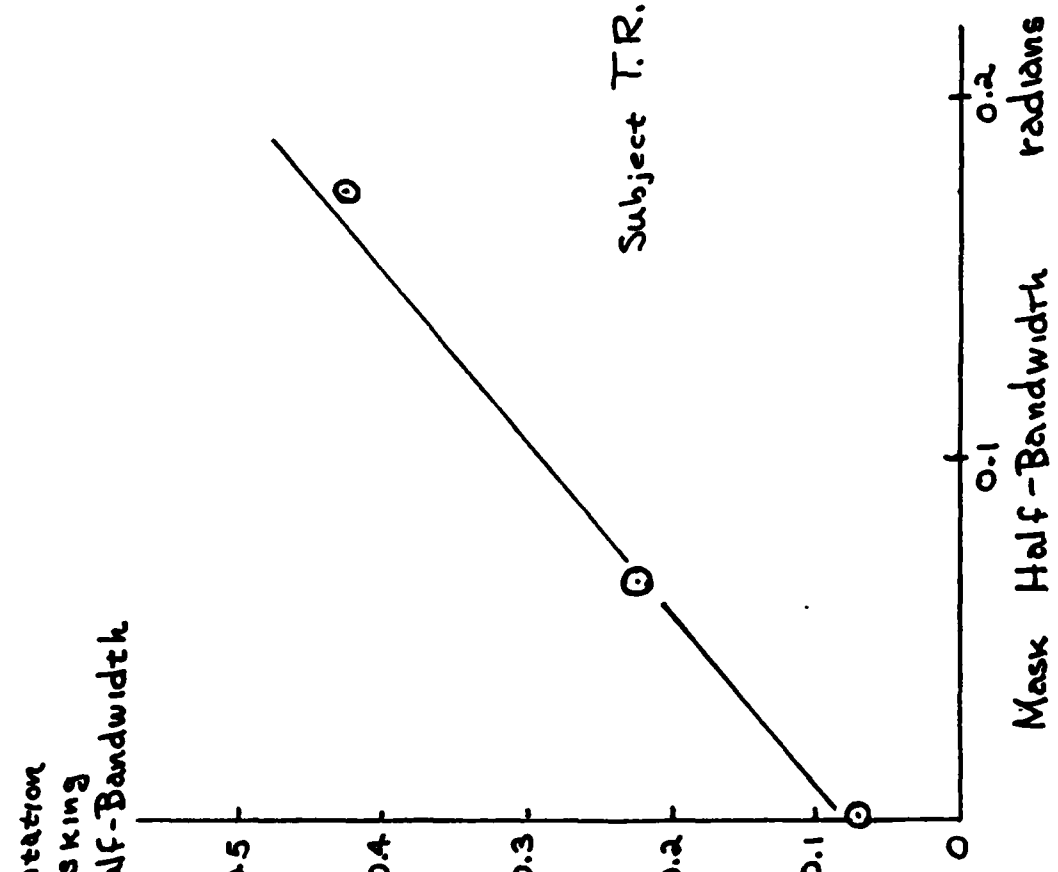
Orientation
Masking
Half-Bandwidth
radians
0.5
0.4
0.3
0.2
0.1
0
0.1
0.2
Mask Half-Bandwidth radians
Subject T.R.

FIGURE 8.

from the mask. If this view is correct, then the masking tuning function would be expected to broaden with the bandwidth of the BLPS mask, since the *mask itself* would then contain many beats, thus rendering the beat caused by the test less effective in identifying the presence of the test. This result was confirmed (Figure 8). Note that the masking tuning curve increases approximately in proportion to the mask bandwidth, for the several values tested with a proportionality factor of 2. This tells us that the test must be twice as far removed from the centroid of the BLPS mask as the boundary enclosing the BLPS components. Our interpretation of this result is that the half-bandwidth of the mask defines the bandwidth of the *beats* which appear in the complicated mask image while the spectral distance between the test grating and the mask centroid defines the new beats introduced into the combined mask and test image by the test. These new beats must be twice as high in spatial frequency as the beats of the mask itself in order for the test to become much more detectable.

In summary, incoherent masking with BLPS masks is exceptionally strong, with strength varying inversely with mask bandwidth. Masking is about equally strong for stationary or shimmering masks. When the incoherent mask bandwidth is very small, a test can become highly visible when only slightly different from the mask, presumably because the test produces a beat that is highly detectable. As the mask bandwidth broadens, the masking tuning broadens since the beats produced by the test are obscured by those already in the mask, and the test becomes

visible only when of a much higher spatial frequency. The results strongly suggest then, that the high masking effectiveness of BLPS masks of moderate bandwidth results from their ability to obscure beats that would otherwise be visible when the test is presented. Note that the beats in these images are nonspectral and are perceived only by a nonlinear operation in the visual signal processing system. This says that the entire masking and detection process for these band limited images cannot be explained by linear mechanisms. An interesting feature of the results is the data collapses better across observers using absolute test contrast (not masking factor). This indicates unmasked test sensitivities are irrelevant to the detection process with the mask. Some data for a third observer taken with 7% contrast mask (not 11% as reported here) show a Weberian function (where test contrast is proportional to mask contrast), which supports the beat detection interpretation.

REFERENCES

Blakemore, C. and Campbell, F.W. (1969). On the existence of neurons in the human visual system selectively sensitive to the orientation and size of retinal images. *J. Physiol.* **203**, 237-260.

Burbeck, C.A. and Kelly, D.H. (1981). Contrast gain measurements and the transient/sustained dichtomy. *J. opt. Soc. Am.* **71**, 1335-1342.

Campbell, F.W. and Kulikowski, J.J. (1966). Orientational selectivity of the human visual system. *J. Physiol.* **187**, 437-445.

Daugman, J.G. (1984). Spatial visual channels in the Fourier plane. *Vision Res.* **24**, 891-910.

Daugman, J.G. (1985). Uncertainty relation for resolution in space, spatial frequency, and orientation optimized by two-dimensional visual cortical filters. *J. opt. Soc. Am.* **2:7**, 1160-1169.

Gabor, D. (1946). Theory of communication. *J. Inst. Elect. Eng.* **93**, 429-457.

Gilinsky, A.S. (1968). Orientation-specific effects of patterns of adapting light on visual acuity. *J. opt. Soc. Am.* **58**, 13-18.

Kronauer, R.E. and Zeevi, Y.Y. (1985). Reorganization and diversification of signals in vision. *IEEE Trans. on Systems, Man and Cybernetics* **15**, 91-101.

Legge, G.E. and Foley, J.M. (1980). Contrast masking in human vision. *J. opt. Soc. Am.* **70**, 1458-1471.

Levinson, E. and Sekuler, R. (1975). The independence of channels in human vision selective for direction of motion. *J. Physiol.* **250**, 347-366.

Pantle, A. and Sekuler, R. (1968a). Size-detecting mechanism in human vision. *Science* **162**, 1146-1148.

Pantle, A. and Sekuler, R. (1968b). Velocity-sensitive elements in human vision: Initial psychophysical evidence. *Vision Res.* **8**, 445-450.

Sekuler, R.W. and Ganz, L. (1963). Aftereffect of seen motion with a stabilized retinal image. *Science* **139**, 419-420.

Stromeyer, C.F. III, Kronauer, R.E., Madsen, J.C., and Klein, S.A. (1984). Opponent movement mechanisms in human vision. *J. opt. Soc. Am.* **A**, **1**, 876-884.

Stromeyer, C.F. III and Julesz, B. Spatial-frequency masking in human vision: critical bands and spread of masking. *J. opt. Soc. Am.* **62**, 1221-1232.

LIST OF ENCLOSED REPRINTS OF RESEACH SUPPORTED BY CONTRACT

Daugman, J.G. (1983). Visual plascitity as revealed in the two-dimensional modulation transfer function of a meridional amblyope. *Human Neurobiology* **2**, 71-76.

Daugman, J.G. (1983). Six formal properties of anisotropic visual filters: Structural principles and frequency/orientation selectivity. *IEEE Transactions on Systems, Man, and Cybernetics* **13**, 882-887.

Daugman, J.G. (1984). Spatial visual channels in the Fourier plane. *Vision Res.* **24**, 891-910.

Daugman, J.G. (1985). Uncertainty relation for resolution in space, spatial frequency, and orientation optimized by two-dimensional visual cortical filters. *J. opt. Soc. Am.* **2**:7, 1160-1169.

Green, M., Chilcoat, M. and Stromeyer C.F. III (1983). Rapid motion aftereffects seen within uniform flickering test fields. *Nature* **303**, 61-62.

Kronauer, R.E. and Zeevi, Y.Y. (1985). Reorganization and diversification of signals in vision. *IEEE Trans. on Systems, Man, and Cybernetics* **15**, 91-101.

Stromeyer, C.F. III, Kronauer, R.E., Madsen, J.C. and Klein, S.A. (1984). Opponent movement mechanisms in human vision. *J. opt. Soc. Am.* **A**, **1**, 876-884.

LIST OF TITLES OF TALKS ON RESEARCH SUPPORTED BY CONTRACT

Daugman, J.G., Kronauer, R.E. and Zeevi, Y.Y. (1982). Perceived randomness in images with sparse punctate two-dimensional spectra. Euorpean Conference on Visual Perception, Leuven, Belgium, Sept. 1982. *Perception* **11(1)**, A22.

Daugman, J.G. (1983). The visual spatio-temporal 'missing fundamental' and product image representations. ARVO, May 1983.

Daugman, J.G. (1983). Efficiency of visual mechanisms in the two-dimensional spatial and Fourier planes. Troisieme Seminaire Hivernal Des Neurosciences Europeenes, Les Arcs, France, May 1983.

Daugman, J.G., Kronauer, R.E., and Zeevi, Y.Y. (1984). Perception of two-dimensional phase modulation and amplitude modulation signals in spatio-temporal band-limited textures. Seventh European Conference on Visual Perception, Cambridge, United Kingdom, Sept. 1984. *Perception* **13**, A16.

Daugman, J.G., Kronauer, R.E., and Zeevi, Y.Y. (1984). Supermasking by bandlimited dynamic incoherent images. ARVO, May 1984.

Daugman, J.G. (1985). Image analysis by local two-dimensional spectral signature. (Invited Paper). *J. opt. Soc. Am.* **2:10**.

Daugman, J.G. and Kronauer, R.E. (1985). Image analysis and efficient reconstruction by simulated neural primitives. Eighth European Conference on Visual Perception, Peniscola, Spain, Sept. 1985. *Perception* **14**, A34, (1985).

Kronauer, R.E., Zeevi, Y.Y. and Daugman, J.G. (1982). Degree of disorder perceived in images with punctate spectra. *J. opt. Soc. Am.* **72**, 1798.

Kronauer, R.E., Daugman, J.G., Zeevi, Y.Y. and Namioka, M.E. (1983). Fourier synthesis of spatio-temporal textures: Perceptual complexity, coherence and chaos. ARVO, May 1983.

Kronauer, R.E., Zeevi, Y.Y., and Daugman, J.G. (1984). Masking tuning properties of dynamic sine-wave gratings are anomalous for 'channels' theory. Seventh European Conference on Visual Perception, Cambridge, United Kingdom, Sept. 1984.

Kronauer, R.E., Daugman, J.G. and Zeevi, Y.Y. (1984). Masking tuning distribution in 3-D spatio-temporal frequency space. ARVO, May 1984.

Kronauer, R.E., Daugman, J.G., and Zeevi, Y.Y. (1984). Chaos and order in the perception of bandlimited dynamic textures. Extraction of local spectral signatures. Systems Approach to Vision (Workshop), Amsterdam, Aug. 1984.

Zeevi, Y.Y., Kronauer, R.E., and Daugman, J.G. (1982). Spatio-temporal masking: Asymmetry, nonseparability, and facilitation, ARVO, May 1982.

END

FILMED

6-86

DTIC